3D Kriging interpolation for traffic noise visualization: designing noise observation points and valuation of spatial interpolation accuracy

N Wickramathilaka[1, 2], U Ujang[1]
[1] 3D GIS Research Lab, Faculty of Built Environment and Surveying, Universiti Teknologi Malaysia, 81310, Johor Bahru, Johor, Malaysia
[2] Southern Campus, General Sir John Kotelawala Defence University, Edison Hill, Nugegalayaya, Sewanagala, Sri Lanka
E-mail: nevilvidyamanee@kdu.ac.lk

Abstract. Identifying the risk of traffic noise is vital in minimizing traffic noise pollution in urban areas. As noise travels in every direction, 3D visualization of traffic noise is essential, which involves visualising traffic noise along the facades of buildings. A standard traffic noise model is necessary to calculate traffic noise levels, as several factors affect traffic noise. Moreover, designing noise observation points in 3D and spatial interpolation play significant roles in 3D noise visualisation. Therefore, this study demonstrates the results by elaborating on the spatial interpolation and designing noise observation points. A noise observation point consists of four parameters in 3D space. Generally, Inverse Distance Weighted (IDW), Triangular Irregular Network (TIN), and Kriging do not support the interpolation of four parameters in 3D. However, 3D Kriging in Empirical Bayesian Kriging provides significant opportunities to interpolate noise levels in 3D. However, the elements of the function of spatial interpolations are vital for accuracy. The 3D Kriging uses different variograms according to semivariance. This variogram directly impacts the weighting factor of 3D Kriging. Therefore, this study develops a comparison to identify the impact of different variograms on the accuracy of 3D Kriging interpolation on traffic noise.

1. Introduction

Road traffic noise pollution is 90% of noise pollution in urban cities, while the other 10% comes from industrial and commercial proceedings [1,2]. Traffic noise pollution depends not only on the vehicles and flow of traffic [3,4]. Several physical and environmental factors are affected by traffic noise pollution. The number of vehicles, the type of the vehicles, the speed of vehicles, noise reflectance of buildings and barriers, noise absorption by the ground, and weather conditions are the main influences on the visualisation of traffic noise [5,6,7]. Therefore, a standard traffic noise equation is the main one to identify traffic noise levels [8]. Collecting noise levels in everywhere is not a possible task, and it may be time-consuming task [5,7]. Therefore, adopting spatial interpolation is prominent to visualise traffic noise levels in 3D space. Extending from 2D to 3D is a need for advanced spatial applications [9,10,11]. In particular, 3D traffic noise visualisation is integrated with a 3D building model and noise is visualised along the facades of the buildings [12,13]. The design of 3D building models and the design of noise observation points (Nops) along the facades are the main components of spatial interpolations [14]. In particular, a simple building model, such as Level of details (LoD1) is enough to visualise 3D traffic noise along the facades of buildings [15,16]. 3D noise contours and 3D voxels are vital for visualising traffic noise levels in 3D [17]. However, there is an issue of visualising traffic noise using voxels using IDW, TIN, and Kriging [18]. However, combining the multidimensional geostatistical layer of 3D Kriging gives a significant access to visualise traffic noise levels using 3D voxels [19].

1.1. 3D Kriging

Kriging is a geostatistical method. It means that correlation of observed values is taken as a quantity. Kriging is vital for interpolating clustered data and a large size of data [20]. The correlation of observed points denoted by the semivariance. Semivariance is the decrease of the similarity of the interpolated values with the observed values with the distance [21]. The fitted model for this semivariance is called a variogram. Furthermore, the surface of the Kriging interpolation depends on which variogram is selected for the function of spatial interpolation as well as number of points and the search radius [22]. 3D Kriging is an Empirical Bayesian Kriging, this means, error of the variogram is automatically calculated during the process. Not like 2D Kriging, the 3D Kriging supports interpolating 4 parameters in a 3D space. It means that multidimensional 3D Kriging generates 3D geostatistical layers along the vertical direction [23]. Thus, 3D Kriging is vital to interpolating Nops in 3D space. Moreover, Empirical Bayesian Kriging is performed by embedding with environment using the geostatistical wizard. Throughout the process, input points, configure parameters, and cross-validation (prediction error) of interpolated surface and input points are vital. This process investigates the cross-validation (prediction error) of results is the same as empirical Bayesian Kriging in 2D. The 3D Kriging facilities allow geostatistical layers along the vertical axis by changing the z coordinate [24]. Thus, this scenario can be adopted to interpolate Nops along the vertical direction. Figure 1 shows that the 3D Kriging geostatistical layers move in the vertical direction [23].

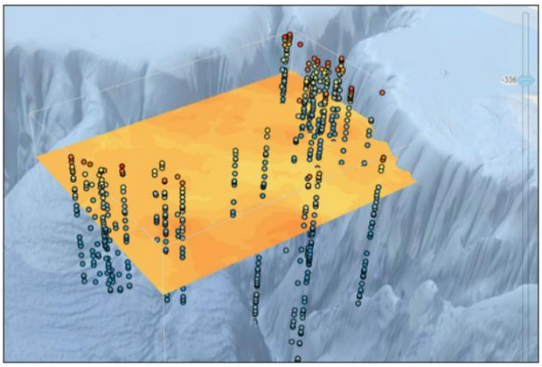

Figure 1. Geostatistical layers in 3D are visualised as 2D transects.

1.2. Elements of 3D Kriging

The vertical and horizontal movements in the data values of the environmental process is vital for 3D Kriging. Furthermore, these moments change slowly along the same elevation [21]. However, it changes quickly as the elevation decreases or increases. Therefore, interpolating road traffic noise levels in 3D is applicable for 3D Kriging. In this case, to predict a new value, how data values move vertically and horizontally, an elevation inflation factor. This means that the horizontal coordinates the same and the points are stretched along the vertical axis [23]. Then, to make the values for the unknown, the stretched coordinates are used. If no inflation factor is provided, a value will be determined using the maximum likelihood method during the processing time. The aim is to select an inflation factor in which the observed values of the stretched points change at the same horizontal as vertical rate [23]. Figure 2 illustrates the stretching of points in 3D [23]. Furthermore, stretching the values along the vertical direction like this allows us to estimate the semivariogram and assign correct weights [25]. Moreover, vertical trend removal is also vital in 3D Kriging. The order of the trend removal parameter can be adopted to eliminate the linear trend in the vertical direction [23,26]. When the elevation inflation factor focusses on the rapidly changing values along the vertical direction, the linear trend corrects for changing values of data as the elevation decreases or increases. Generally, order one of polynomial [27].

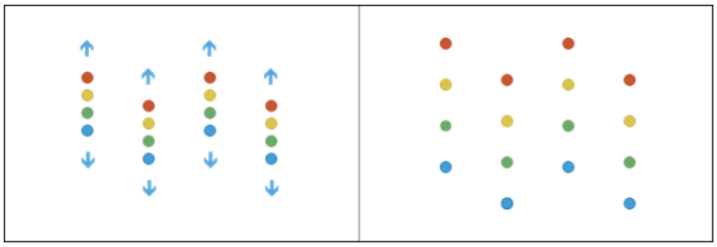

Figure 2. Points stretched in 3D.

1.3. Variograms of 3D Kriging

The semivariance of observed points (known points) is considered in 3D Kriging [21]. The model fitting for this semivariance is called selecting a variogram for that. However, the error of the variogram (model fitting) is automatically calculated in 3D Kriging. Power, linear, thin plate spline, exponential, whittle, and k-Bessel are the main variograms used in 3D kriging [22]. Therefore, identifying the best variogram is vital for interpolating values in any geographical application. There are two Kriging methods: universal Kriging and ordinary Kriging. In universal Kriging, it shows this scientific justification. This means that universal Kriging is only used when there is a trend in a data and if scientific justification can be made. For example, if it considers modelling air pollution modelling by a deterministic function by a polynomial [28]. The original measured points are subtracted by this polynomial function, and the correlation is modelled from random errors. When the model is fitted to the random errors before performing the interpolation, the polynomial function is added back to the interpolation to show accurate results. However, ordinary Kriging is widely used for spatial interpolation. It assumes a constant mean for the unknown value [20]. However, this assumption is a reasonable unless there is a scientific rejection. Identifying the best suitable 3D Kriging variogram is vital for any application. This study is conducted to identify the best suitable Kriging for visualising road traffic noise in 3D space. The main objective of this study is to identify the performance of 3D Kriging for traffic noise visualisation in 3D.

2. Methodology

2.1. Study Area

This study is carried out to identify the performance of 3D Kriging for traffic noise visualisation. In particular, the influence of the variogram on the accuracy of the 3D Kriging interpolation on the interpolation of road traffic noise levels was examined. This study's scope is restricted to assessing how different variograms affect accuracy. As a result, the number of points and the search radius are taken as constants. However, noise observation locations are designed along building facades as grids, and the spacing between each noise observation point is 2 metres, in order to maximize the accuracy of the interpolation and visualization. In this study, a part of the inner circle area of Universiti Teknologi Malaysia (UTM) was selected, which is located around the science faculty area. The location coordinates of the study area are at 1°33'37.6"N 103°38'16.4" E and are located at UTM, Johor, Malaysia. Figure 3 illustrates the overview of the study area. According to previous studies and the verifications field, there are higher levels of noise during the morning period. The study workflow is shown in Figure 4.

Figure 3. Overview of the study area (source: Google Earth).

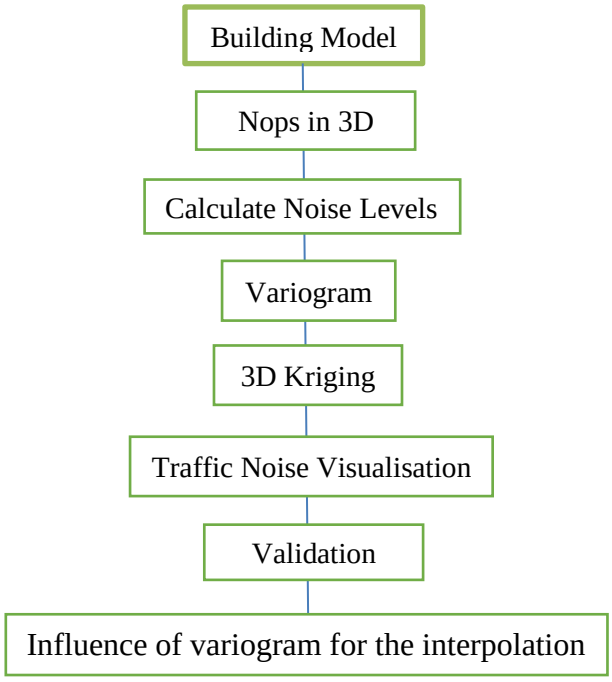

Figure 4. Workflow of the study.

2.2. Building model

The 3D building model was created by drone point clouds. Point clouds have been utilised in many 3D city modelling research starting from data acquisition, modelling, and applications [29,30,31,32]. In this research, a simple building model is used to visualise the noise level of road traffic. Therefore, the level of details (LOD1) was used to build the modelling. Noise observation points (Nops) were designed in a 3D space along the facades of the buildings. The Nops were designed as vertical grids, and the distance interval between the Nops is 2 metres. The designed Nops are shown in Figure 5.

2.3. Calculate the noise levels

For road statistical data, the number of vehicles for each category such as light, medium, and heavy vehicles was collected by manually. The average speed of the vehicles was taken for each category. All statistical data were collected from 7.30 am to 9.30 am on ten mornings due to there being a higher

traffic flow during this time. Traffic noise levels were calculated to the Nops using the Henk de Kluijver road traffic noise equation. The equation of Henk de Kluijver is shown in Equation 1 [14].

$$L(dB) = E + C_{optrek} + C_{reflectie} - D_{afstand} - D_{lucht} - D_{bodem} - D_{emote} - D_{barrier} \quad (1)$$

L(dB) is the traffic noise level. E is the traffic noise emission level. To calculate the value for the E, the speed of vehicles, the type of vehicles (light, medium, and heavy) and the number of vehicles should be observed in heavy traffic flow. C_{oprek} is the extra noise emission from accelerating and braking. $C_{reflectie}$ is the noise reflection of barriers and buildings. Moreover, noise reflection can be calculated by Equation (2).

$$C_{reflectie} = 1.5*Fobj \quad (2)$$

Fobj is between 0 and 1, and it can be calculated from (θ'/θ). The θ' is the sum of angles subtended from opposite side buildings and barriers, and θ is the total subtended angle [14]. The reason is being, the buildings are located continuously in the selected area, and the ratio of θ and θ' was assumed to equal 1. Therefore, noise reflection was taken as 1.5 dB. Equation (3) describes the D_{bodem}.

$$D_{bodem} = B\,[2+4(1-e-0.04r)*(e-0.65h_w + e-0.65(h_{weg}-0.75)] \quad (3)$$

The h_{weg} is the elevation of the road from reference ground level and the h_w is the elevation of the Nops from the reference ground level. B is the road traffic noise absorption coefficient by ground. The B is 1 for the completely covered grass, and for hard ground, the B is 0 [33]. B is 0.3 for the gravel grounds [34]. The ground of the study area covered by grass ground and hard ground. Therefore, the noise absorption coefficient of hard ground and grass ground was taken, respectively, to be 0 and 1. D_{meteo} represents noise reduction due to wind conditions. Equation (4) shows that. Noise mitigation by barriers was not considered for the calculations.

$$D_{meteo} = 3.5-3.5e\ (-0.04r/\ (h_{weg}+h_w+0.75))\ (1.9) \quad (4)$$

2.4. 3D Kriging and validation

3D Kriging in Empirical Bayesian Kriging was used to interpolate road traffic noise levels in 3D space. 3D Kriging provides facilities to interpolate four parameters in a 3D space. Furthermore, it provides horizontal geostatistical layers along the vertical axes [23]. Thus, 3D Kriging provides 3D geostatistical layers for 3D Nops. As elements of 3D Kriging, different variograms were used to check the accuracy of the interpolation [35]. However, the elevation inflation factor was taken as default. This means that, during processing time according to the Nop value range of Nops, the software assigns the inflation factor using maximum likelihood. Moreover, the order of trend removal was taken as 1st order. However, these 3D Kriging layers were combined with 3D voxels to visualise traffic noise levels in 3D [26]. The voxels size was 0.5 metres. To verify the precision of the visualisation, the Root Mean Square Error (RMSE) was utilised. Sound Level Meters (SLM) were set up in the building corridors. This indicates that the first and second floors, as well as the second and third levels' margins, were formed by SLM. The DEKKO SL-130 sound level metre was employed. The accuracy of this noise meter is 0.1 dB, and noise levels were measured at ten (10) different locations. The recorded dB levels occurred during perpendicular propagation from the road's centre line to the receiver. From 7.30 to 9.30 am on ten mornings, noise levels were measured and average noise levels were recorded at twenty (10) different sites. The noise levels at each of the ten (10) 3D voxel sites were then compared.

3. Results and Discussion

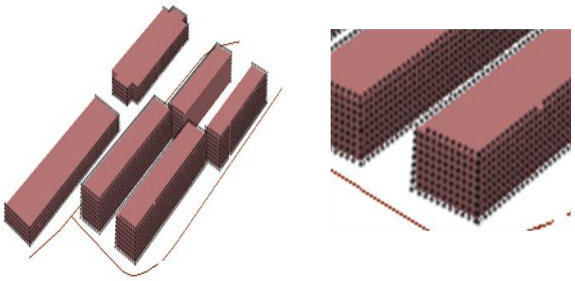

Figure 5. Designing of noise observation points along the facades of buildings.

Table 1. RMSE of different variograms.

Variogram	RMSE
Power	1.337
Linear	2.32
Thin plate spline	1.856
Exponential	1.724
Whittle	1.366
K-Bessel	1.126

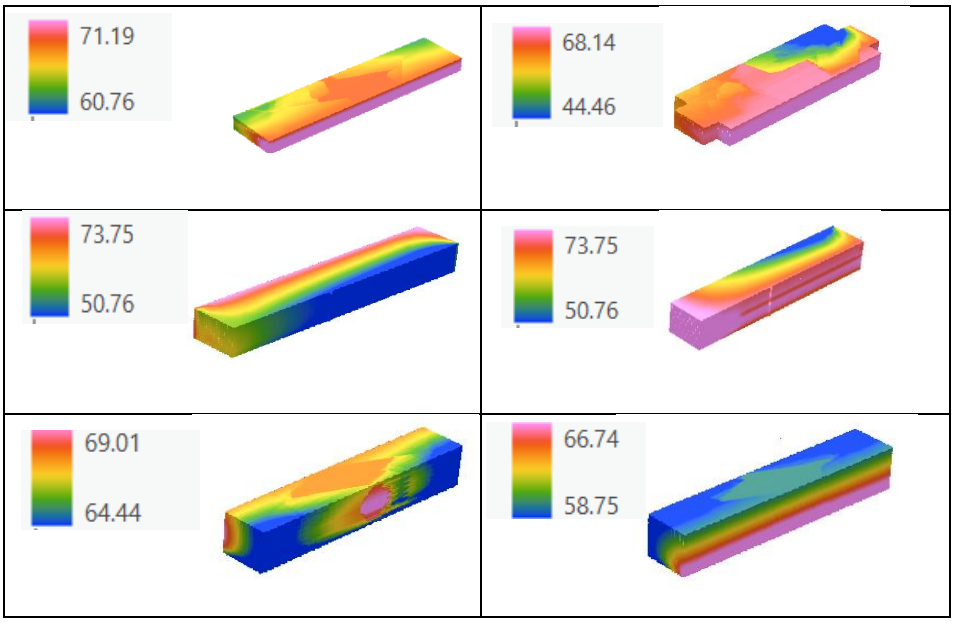

Figure 6. 3D Kriging K-Bessel variogram of road traffic noise voxels.

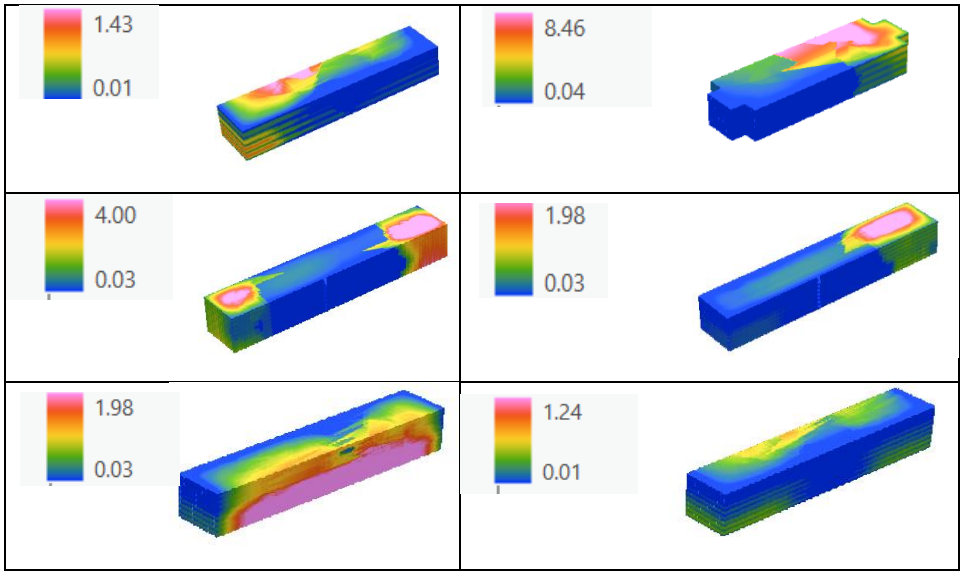

Figure 7. Standard error of 3D Kriging K-Bessel variogram voxels.

The precision of the 3D interpolation of road traffic noise is used in the 3D Kriging. The autocorrelation of the observed points is taken into account in 3D kriging. By using semivariance, this autocorrelation is measured. The variogram, which has a decreasing correlation of points with distance, is the fitting model for this semivariance. To fit the variogram model, there are important equations. As a result, these variograms affect how accurate 3D kriging interpolation is. The variogram can be fitted to the semivariance under the noise levels of Nops. Therefore, identifying the performance of the variogram is vital for 3D interpolation. The 3D noise voxel denotes a 3D pixel of noise. Therefore, it is crucial to extract front-pixel noise from roadways to identify road traffic noise levels along the facades of buildings. Designing Nops with 2 metres distance is vital for the accuracy of the 3D interpolation. According to the Henk de Kluijver road traffic noise model, the noise will decrease approximately 1dB (A) while propagating 2 metres. Thus, maintaining a distance of 2 metres for Nops is prime. 3D Kriging creates multidimensional 3D geostatistical layers between each set of Nops along the vertical direction. The RMSE value of the variograms using 3D Kriging interpolations and sample noise measurements is shown in Table 1. For the 3D road traffic noise interpolation, the K-Bessel variogram of 3D Kriging produces a lower RMSE value and the linear variogram gives a higher RMSE value. Therefore, the K-Bessel variogram of 3D Kriging voxels was used to visualise final noise levels of selected buildings. Figure 6 shows the 3D road traffic noise from the K-Bessel 3D Kriging voxels. K-Bessel variogram processing takes longer than other variograms. Additionally, a linear variogram processes data faster than other variograms. Power and Whittle variograms provide average accuracy for interpolation. Standard error can occur in the predictions. This means that the predicted surface 100% does not coincide for the observation points. Then there is a standard error for the predictions. This standard error is not a constant for the interpolated surface. Generally, identifying this standard error can be called cross-validation of the interpolated surface (error of predicted surface and observed points). Thus, the standard error for the prediction of the K-Bessel variogram interpolation is shown in Figure 7. According to Figure 7, the standard error is higher when increasing the LoD (Level of Details) of the building.

4. Conclusions

3D kriging offers the ability to interpolate four parameters in a 3D space, unlike conventional 2D spatial interpolations. In other words, 3D kriging generates 3D geostatistical layers that act as horizontal planes along the vertical axis. Furthermore, by mixing these geostatistical layers, 3D voxels can be produced. Additionally, because 3D kriging uses empirical Bayesian kriging, the error of its variograms is estimated automatically as it is processed. As a result, 3D kriging is essential for interpolating four parameters, such as noise observation locations along building facades. The design of building models, the design of noise observation points (Nops), the calculation of traffic noise levels, and the 3D spatial interpolation are vital to the visualisation of 3D road traffic noise. The accuracy of the depiction of road traffic noise depends on the representation of the building model in a 3D environment. Urbanised places have many intricately designed buildings. On the side of the road, one structure may be hidden by another. Therefore, this structure could serve as a noise barrier. Therefore, when calculating noise levels, the noise propagation path should be taken into account. It implies that the real noise propagation path and building barriers may differ. To visualise the levels of road traffic noise along the facades of the buildings, it is also important to take into account the design of the structures. The distance between the noise observation locations on the façade and the noise source might induce fluctuations in road traffic noise levels along their curving surfaces. Nops consists of four parameters in a 3D space. Therefore, the IDW, Kriging, and TIN spatial interpolation cannot be used directly to interpolate road traffic noise levels in 3D space due to this interpolation directly supporting the interpolation of 3 parameters. Furthermore, development for spatial interpolation should be inserted for these spatial interpolations. However, 3D Kriging can be applied to eliminate the above-mentioned issues. Moreover, 3D kriging can be combined with 3D voxels. Therefore, 3D kriging is vital to visualise. The K-Bessel variogram of 3D kriging provides higher accuracy for 3D surfaces. However, demonstration of the standard prediction error for any interpolated surface is crucial to understand the distribution of prediction error of any interpolation. Furthermore, the type of transformation, subset size, and order of trend removal were not changed during the processing of this study. It can be suggested to identify the performance of 3D Kriging with these elements. 3D visualisation of traffic noise levels along the facades of the buildings, it is possible to detect noise levels. The World Health Organization (WHO) states that the maximum permissible level of traffic noise is 55 dB (A). Therefore, urban planners can gain insight into the noise pollution of urban areas through the 3D depiction of road traffic noise. To reduce the noise pollution caused by vehicle traffic, it has been suggested in a number of earlier studies to build tree belts around roadways. Moreover, this sample study's findings can be used to metropolitan areas to further evaluate the 3D visualisation's accuracy. Future recommendations include comparing the accuracy of the visualization with other road traffic models, including the CNOSSOS-EU model of the European Union, the Federal Highway Administration traffic noise model (FHWA), the road traffic noise model (CoRTN) in the United Kingdom, and the RLS-90 model of Germany. Furthermore, while RMSE is a common validation method, the use of multiple validation methods could provide a more robust assessment of the accuracy of the 3D Kriging method. The findings of this work can be applied to a variety of geoscience applications that include four characteristics (a location and a geoscience incident value), such as 3D visualization of air pollution and 3D visualization of subsurface water quality.

Acknowledgments

This research was supported by Ministry of Education (MOE) through Fundamental Research Grant Scheme (FRGS/1/2021/WAB07/UTM/02/2).

References

[1] Yang, W., He, J., He, C. and Cai, M. (2020) '' Evaluation of urban traffic noise pollution based on noise maps', Transportation Research Part D: Transport and Environment. Elsevier, 87, p. 102516.
[2] Peng, J., Parnell, J. and Kessissoglou, N. (2021) '' Spatially differentiated profiles for road traffic noise pollution across a state road network', Applied Acoustics. Elsevier Ltd, 172, p. 107641.
[3] Huh, S. Y. and Shin, J. (2018) '' Economic valuation of noise pollution control policy: does the type of noise matter? ', Environmental Science and Pollution Research. Environmental Science and Pollution Research, 25(30), pp. 30647–30658.
[4] Gilani, T. A. and Mir, M. S. (2021) '' Modelling Road traffic noise under heterogeneous traffic conditions using the graph-theoretic approach', Environmental Science and Pollution Research. Environmental Science and Pollution Research, 28(27), pp. 36651–36668.
[5] Munir, S. et al. (2021) '' Temporal and seasonal variations of noise pollution in urban zones: a case study in Pakistan', Environmental Science and Pollution Research, 28(23), pp. 29581–29589.
[6] Partheeban, P. et al. (2021) '' Urban Road traffic noise on human exposure assessment using geospatial technology', Environmental Engineering Research, 27(5), pp. 210249–0.
[7] Rey, G. and Gómez, V. (2021) '' Uncertainty evaluation of road traffic noise models in two Ibero- American cities', Applied Acoustics, 180, p. 108134.
[8] Debnath, A. and Singh, P. K. (2018) '' Environmental traffic noise modelling of Dhanbad township area-A mathematical based approach', Applied Acoustics, 129, pp.
[9] Azri, S., Ujang, U., Anton, F., Mioc, D., Rahman, A.A. (2016a) '' 3D Nearest Neighbour Search Using a Clustered Hierarchical Tree Structure'. Int. Arch. Photogramm. Remote Sens. Spatial Inf. Sci. XLI-B2, 87-93.
[10] Azri, S., Ujang, U., Rahman, A.A., Anton, F., Mioc, D. (2016b) ''3D Geomarketing Segmentation: A Higher Spatial Dimension Planning Perspective'. Int. Arch. Photogramm. Remote Sens. Spatial Inf. Sci. XLII-4/W1, 1-7.
[11] Hairuddin, A., Azri, S., Ujang, U., Cuétara, M.G., Retortillo, G.M., Mohd Salleh, S. (2019) '' Development of 3D City Model Using Videogrammetry Technique'. Int. Arch. Photogramm. Remote Sens. Spatial Inf. Sci. XLII-4/W16, 221-228.
[12] Peng, J., Bullen, R. and Kean, S. (2014) '' The effects of vegetation on road traffic noise', Internoise 2014 - 43rd International Congress on Noise Control Engineering: Improving the World Through Noise Control, pp. 1–10.
[13] Alomía, G., Loaiza, D., Zúñiga, C., Luo, X. and Asorey-Cacheda, R. (2021) '' Procedural modeling applied to the 3D city model of bogota: a case study', Virtual Reality and Intelligent Hardware, 3(5), pp. 423–433.
[14] Ranjbar, H. R., Gharagozlou, A. R., Reza, A. and Nejad, V. (2012) '3D Analysis and Investigation of Traffic Noise Impact from Hemmat Highway Located in Tehran on Buildings and Surrounding Areas', 2012(August), pp. 322–334.
[15] Kumar, K., Ledoux, H., Commandeur, T. J. F. and Stoter, J. E. (2017) '' Modelling urban noise in City GML ADE: case of the Netherlands', ISPRS Annals of the Photogrammetry, Remote Sensing and Spatial Information Sciences, 4(4W5), pp. 73–81.
[16] Saran, S., Oberai, K., Wate, P., Konde, A., Dutta, A., Kumar, K. and Senthil Kumar, A. (2018) '' Utilities of virtual 3D city models based on CityGML: various use cases', Journal of the Indian Society of Remote Sensing. Springer India, 46(6), pp. 957–972.
[17] Alcaras, E., Amoroso, P. P. and Parente, C. (2022) '' The influence of interpolated point location and density on 3D bathymetric models generated by Kriging methods: An Application on the Giglio Island Seabed (Italy) ', Geosciences (Switzerland), 12(2).

[18] Comber, A. and Zeng, W. (2019) '' Spatial interpolation using areal features: A review of methods and opportunities using new forms of data with coded illustrations', Geography Compass, 13(10), pp. 1–23.
[19] He, L., Zhang, J., Chen, S., Hou, M. and Chen, J. (2022) '' Three-dimensional hydrogeological modeling method and application based on TIN-GTP-TEN', Earth Science Informatics. Springer Berlin Heidelberg, 15(1), pp. 337–350.
[20] Zhang, Y., Ji, W., Saurette, D. D., Easher, T. H., Li, H., Shi, Z., Adamchuk, V. I. and Biswas, A. (2020) '' Three-dimensional digital soil mapping of multiple soil properties at a field-scale using regression kriging', Geoderma. Elsevier, 366(January 2019), p. 114253.
[21] Venkataraman, S. and Falls, S. (2005) '' Voxel-based analysis and visualization of rainfall data'.
[22] Izady, A., Abdalla, O., Ahmadi, T. and Chen, M. (2017) '' An efficient methodology to design optimal groundwater level monitoring network in Al-Buraimi region', Oman, Arabian Journal of Geosciences. Arabian Journal of Geosciences, 10(2).
[23] Esri (2020) What is Empirical Bayesian Kriging 3D?
[24] Sabine Grunwald, Phillip Barak and Dan Rooney (2013) 'Web-Based Virtual Models for the Earth Science Community', (January 2001).
[25] Rahimi, H., Asghari, O., & Afshar, A. (2018). A geostatistical investigation of 3D magnetic inversion results using multi-Gaussian kriging and sequential Gaussian co-simulation. Journal of Applied Geophysics, 154, 136–149.
[26] Li, J., Liu, P., Wang, X., Cui, H. and Ma, Y. (2022) '' 3D geological implicit modeling method of regular voxel splitting based on layered interpolation data', Scientific Reports. Nature Publishing Group UK, 12(1), pp. 1–14.
[27] Zelt, C. A., Azaria, A. and Levander, A. (2006) '' 3D seismic refraction travel time tomography at a groundwater contamination site', Geophysics, 71(5).
[28] Feng, D., Hu, K., Li, H., Yun, A., & Li, B. (2015). Three-Dimensional Mapping of Soil Organic Carbon by Combining Kriging Method with Profile Depth Function. PLOS ONE, 10(6), e0129038.
[29] Ahmad, N., Azri, S., Ujang, U., Cuétara, M.G., Retortillo, G.M., Mohd Salleh, S. (2019) '' Comparative Analysis of Various Camera Input for Videogrammetry'. Int. Arch. Photogramm. Remote Sens. Spatial Inf. Sci. XLII-4/W16, 63-70.
[30] Hinge, L., Gundorph, J., Ujang, U., Azri, S., Anton, F., Abdul Rahman, A. (2019) '' Comparative Analysis of 3D Photogrammetry Modeling Software Packages for Drones Survey'. Int. Arch. Photogramm. Remote Sens. Spatial Inf. Sci. XLII-4/W12, 95-100.
[31] Ridzuan, N., Ujang, U., Azri, S., Choon, T.L. (2020) '' Visualising Urban Air Quality Using Aermod, Calpuff and CFD Models: A Critical Review'. Int. Arch. Photogramm. Remote Sens. Spatial Inf. Sci. XLIV-4/W3-2020, 355-363.
[32] Sadidi, J., Judaki, Z., Rezayan, H. (2020) '' Designing and implementing a 3D Indoor Navigation Web Application'. jsaeh 7, 67-80.
[33] ISO (1996) '' ISO 9613-2:1996: Acoustics - attenuation of sound propagation outdoors', (1).
[34] Attenborough, K., Bashir, I. and Taherzadeh, S. (2016) '' Exploiting ground effects for surface transport noise abatement', Noise Mapping, 3(1), pp. 1–25.
[35] Krivoruchko, K., & Gribov, A. (2020). Distance metrics for data interpolation over large areas on Earth's surface. Spatial Statistics, 35, 100396.